

Methods

Study subjects

Three pairs of monozygotic twins from the Twin Research Registry at SRI International and three unrelated individuals were included. The protocol was approved by the Stanford University Institutional Review Board, and all participants gave written informed consent. Demographic information is provided in Table 1. All individuals were healthy. None of the individuals had zoster reactivation in the five years prior enrollment, one individual (E) had reactivation more than 5 years ago. All individuals were vaccinated with live attenuated VZV (Zostavax^R, Merck). Peripheral blood was obtained before vaccination and on days 8±1, 14±1 and 28±3 days after vaccination. Blood at similar intervals was also obtained from a control individual who was not vaccinated. Serum samples were obtained before vaccination and on days 1 and 28±3 days after vaccination. Demographic data including HSV and CMV status and humoral and cellular vaccine response is given in Table S1. HSV-1, HSV-2 and CMV status were measured using Focus Diagnostics HerpeSelect 1 ELISA IgG and HerpeSelect 2 ELISA IgG test kits on an Inova Diagnostics Quanta-Lyser at Stanford Health Care Clinical Laboratories. Antibody responses to VZV were determined using the VZV glycoprotein-based Serion ELISA Classic VZV IgG test (Institut Virion\Serion GmbH). Serum samples in duplicate were run according to manufacturer's instructions. All individuals had >100 mIU/ml VZV IgG on prevaccination serum samples, which is considered as seropositive. ELISpot assays were performed using serial dilutions of PBMCs in duplicate on precoated IFN- γ -specific ELISpot plates (Mabtech) and stimulated with 3 μ g/ml VZV lysate for 16 hours. Plates were analyzed using Immunospot software (Cellular Technology Limited). VZV viral lysate from pOKa-infected melanoma MEL39 cells and mock lysate from uninfected MEL39 cells were a gift from Dr. A. Arvin, Stanford. Serum cytokine concentrations were measured using Human 63-plex fluorescent bead assay at Stanford Human Immune Monitoring Center.

Generation of VZV-antigen reactive cells

To obtain VZV-specific CD4 T cells, PBMCs were labeled with CFSE, and ten million cells per culture were stimulated with 3 μ g/ml VZV viral lysate. Control cultures were stimulated with 3 μ g/ml lysate of non-infected cells. In pilot studies, we determined that proliferating T cells were first detected on days 3 and 4 after stimulation and optimal separation of proliferating and non-proliferating cells were obtained after 7-8 days of culture.

To confirm that proliferating cells are VZV reactive, CFSE-labeled PBMCs were stimulated with 3 μ g/ml VZV viral lysate. On day 8, cultured cells were harvested; non-T cells from fresh PBMCs of the same individuals were isolated by negative selection using anti-CD3 magnetic microbeads (Miltenyi Biotec) and labeled with CellTrace Violet (CTV, ThermoFisher Scientific). 1 million of the harvested PBMCs were restimulated with 0.4 million non-T cells and 3 μ g/ml fresh VZV viral lysate for 16 hours. In parallel, harvested PBMCs were restimulated with 50 ng/ml PMA and 500 nM ionomycin. After incubation, cells were stained with AmCyan-anti-CD4 (BD Biosciences), AlexaFluor700-anti-CD8 (BioLegend), APC-Cy7-anti-CD3 (BioLegend) antibodies, and then fixed and permeabilized (BD Cytotfix/Cytoperm kit), followed by staining with APC-anti-TNF α (BD Biosciences), PerCP-Cy5.5-anti-IL2 (BD Biosciences) and PE-anti-IFN γ (eBioscience) antibodies.

To assess VZV-reactivity of naïve T cells, T cells were negatively purified from 10 million PBMCs using EasySep human T cell enrichment kit (StemCell Technologies), stained with PerCP-Cy5.5-anti-CCR7 (BioLegend) and APC-anti-CD45RA (BD Biosciences), followed by cell sorting using a BD Aria 3 cell sorter to obtain naïve T cells (CCR7⁺CD45RA^{high}). Naïve T cells were labeled with CFSE and cultured with 10 million CTV-labeled PBMCs from the same individual and 3 μ g/ml VZV viral lysate. On day 8, cells were stained with anti-CD4, anti-CD8 and anti-CD3 antibodies. Flow cytometric data were collected with a Fortessa flow cytometer and analyzed with Flowjo software (Flowjo, LLC).

For repertoire studies of VZV-reactive T cells, cells were stained on day 8 of culture with Live/Dead Fixable Aqua Dead cell stain dye (Life Technologies), APC-Cy7-anti-CD3 (BioLegend), V450-anti-CD4 (Affymetrix eBioscience) and PerCP-Cy5.5-anti-CD8 antibodies, followed by cell sorting using a BD Aria 3 cell sorter to obtain a minimum of 5,000 and up to 10,000 CD4 T cells (CFSE^{low}CD4⁺CD8⁻CD3⁺) that had divided in response to VZV lysate stimulation. Two to three replicates of PBMC were cultured independently for each prevaccination and postvaccination time point. RNA was prepared using RNeasy micro kit (Qiagen).

For repertoire studies of unstimulated T cells, total CD4 T cells were purified from PBMC using CD4 microbeads and the autoMACS Pro Separator (Miltenyi Biotec). Two replicates of 1x10⁶ CD4 T cells were

collected at each time point. Naïve CD4 T cells ($CD3^+CD4^+CD8^-CCR7^+CD45RA^{high}CD28^+$) and memory CD4 T cells ($CD3^+CD4^+CD45RA^{med/low}$) were collected by cell sorting using FITC-anti-CD3 (BioLegend), V450-anti-CD4 (Affymetrix eBioscience), PE-Cy7-anti-CD8 (BD Biosciences), PerCP-Cy5.5-anti-CCR7 (BioLegend), PE-antiCD28 (BD Biosciences) and APC-anti-CD45RA (BD Biosciences) antibodies. RNA of each T cell population was extracted using AllPrep DNA/RNA mini kit (Qiagen).

Generation of TRB gene library and sequence data analysis

cDNA were prepared from RNA using SuperScript VILO master mix (Invitrogen). The preparation and sequencing of TCRB gene libraries were performed as described (8). Sequencing reads were first filtered by read quality, then assembled and mapped to human TRB reference sequences downloaded from international ImMunoGeneTics (IMGT) information system (<http://imgt.org/>). V, J gene annotation, CDR3 definition and sequencing error correction were performed as described (8). CDR3 out-of-frame sequences were excluded from further analysis.

Identical TCR β chains (clones) were defined as sequences that have the same BV and BJ gene segment and identical CDR3 amino acid sequences. For analysis of TRBV usage, TRBJ usage and CDR3 feature, replicate sequences were collapsed to a single sequence. Sequences that contain ambiguous V genes or J genes were excluded for V and J usage analysis. .

Identification of VZV antigen-reactive TRB sequences

To call a TCR sequence to be derived from a VZV-specific T cell and to exclude contaminating sequences from non-specifically proliferating T cells, we required that (1) the identical sequence was found in at least two independent replicate libraries from the same time point; (2) the frequency of the sequence in the proliferating population was enriched by at least a factor of 2 compared to total CD4 T cells and the enrichment was significant (one-sided Fisher exact test, $q < 0.05$).

Estimation of the genetic influence

TRBV-TRBJ combination usage frequencies were determined after collapsing replicate sequences into a single sequence. Expression patterns between any two individuals were compared using Pearson correlation. Hierarchical clustering was performed based on correlation coefficients. The within twin-pair similarities in TRBV or TRBJ gene usage were determined from the ratio of the average absolute difference in gene frequencies of two unrelated individuals and those within twin-pairs. The nonparametric permutation test was used to test if the average difference within twin-pairs is less than that between unrelated individuals. The overall repertoire similarities of a given cell type between two individuals were expressed as the number of shared TCR β chain sequences divided by the product of the total number of distinct TCR β chain sequences from these two individuals. Similarities between twin-pairs and unrelated individuals were then compared using permutation test.

Estimation of vaccination-induced T cell expansion

To estimate the proportion of clones expanded after the VZV vaccination, we assume a negative binomial model for the count of each clone. Specifically, we denote the count of the j -th clone in i -th replicate at the baseline by n_{ij0} . Similarly, we let n_{ij1} be the count of the j -th clone in i -th replicate at day 8 after vaccination. We assume that

$$n_{ijk} \sim \text{Poisson}(N_{ik}\lambda_{jk}\theta_{ik})$$

$$\theta_{ijk} \sim \text{Gamma}\left(\frac{1}{\sigma_k^2}, \frac{1}{\sigma_k^2}\right)$$

where $i = 1, 2$; $j = 1, \dots, J$, $k = 0, 1$ and N_{ik} is the sequencing depth in the i -th replicate. Our goal is to test the null hypothesis $H_0: \lambda_{j0} = \lambda_{j1}$ and estimate the proportion of clones with $\lambda_{j1} > \lambda_{j0}$. To this end, we consider the test statistics $n_{1j0} + n_{2j0}$. Under the null hypothesis, the conditional distribution

$$n_{1j0} + n_{2j0} | (n_{1j0} + n_{2j0} + n_{1j1} + n_{2j1} = n_j) \sim \text{Binom}\left(n_j, \frac{N_{10}\theta_{1j0} + N_{20}\theta_{2j0}}{N_{10}\theta_{1j0} + N_{20}\theta_{2j0} + N_{11}\theta_{1j1} + N_{21}\theta_{2j1}}\right),$$

$$\theta_{ijk} \sim \text{Gamma}\left(\frac{1}{\sigma_k^2}, \frac{1}{\sigma_k^2}\right).$$

Let \tilde{N}_{j0} denote the null distribution above, which can be easily simulated. Therefore, we may obtain the one-sided mid p-value testing $H_0: \lambda_{j0} = \lambda_{j1}$ vs $H_1: \lambda_{j0} < \lambda_{j1}$ by

$$p_j = \text{Prob}(n_{1j0} + n_{2j0} < \tilde{N}_{j0}) + 0.5 \times \text{Prob}(n_{1j0} + n_{2j0} = \tilde{N}_{j0}).$$

Since we know that under the null distribution the one-sided p-values approximately follow a uniform distribution, we can estimate the proportion of true alternatives as

$$1 - \frac{\sum_j I(p_j > \pi_0)}{(1 - \pi_0)J},$$

where the tuning parameter $\pi_0 \in (0, 1)$ is set as 0.2. To conduct the analysis, one needs to know the value of σ_k^2 , which can be estimated by the moment estimator

$$\hat{\sigma}_k^2 = \frac{\sum_j (n_{1jk}N_{2k} - n_{2jk}N_{1k})^2 - n_{1jk} - n_{2jk}}{2 \sum_j n_{1jk}n_{2jk}N_{1k}N_{2k}}, k = 0, 1.$$

Diversity analysis

The diversity of repertoire was calculated as the number of distinct clones, ordered by decreasing clonal sizes that comprise 80% of repertoire. This metric is unchanged for inferential purposes as the depth of sequencing varies. To study the association of relative change of clones and their sizes, we considered the following regression model:

$$\frac{\lambda_{28jk}}{\lambda_{0jk}} = \alpha_k e^{\beta_k \lambda_{0jk}},$$

$$Y_{28jk} \sim \text{Poisson}(N_{28k} \lambda_{28jk}), \quad Y_{0jk} \sim \text{Poisson}(N_{0k} \lambda_{0jk}),$$

$$\text{and } \beta_k \sim N(\beta_0, \tau^2),$$

where (Y_{0jk}, Y_{28jk}) are observed frequencies for clone j of the k^{th} subject at baseline and day 28, (N_{0k}, N_{28k}) are the observed total frequencies for all clones of the k^{th} subject at baseline and day 28 and $(\lambda_{0jk}, \lambda_{28jk})$ are underlying sizes for clone j of the k^{th} subject at baseline and day 28. Therefore, the parameter β_k represents the association between the relative changes in the clone sizes measured by the ratio $\lambda_{28jk}/\lambda_{0jk}$ and the baseline clone size λ_{0jk} for the k^{th} subject. For example, if β_k is negative, then small clones at the baseline tend to expand less than big clones. β_0 is the population counterpart of β_k and the parameter summarizing the association in the population. To fit this model, we first estimate β_k for each individual and the corresponding standard error is obtained by a parametric bootstrap. We then employ the random effects model used in meta-analysis to obtain the point and interval estimates of β_0 . Due to the small sample size and model-dependent nature of the approach, the results may be sensitive to few influential observations.

Descriptive statistics

The Spearman correlation coefficients between the number of distinct VZV-reactive CD4 TCR β chains and the space taken up by the most abundant clones as well as between the frequencies of VZV antigen-reactive T cells and the richness of their TCR β chain repertoires were estimated. The similarity of TRBV and TRBJ genes frequencies within twin pair and between unrelated individuals were compared using a nonparametric permutation. The frequencies of VZV antigen-reactive TCR β chain sequences in total CD4 T cells and the number of unique VZV-specific TCR β chains before and on days 8, 14, and 28 after vaccination were compared with the paired Wilcoxon-Mann-Whitney test. A p value of 0.05 or less was considered to be statistically significant. All statistical analyses were performed using R3.2.2. (The R Foundation for Statistical Computing, 2015).

Table S1. Demographics of study population.

| Subject ID | Gender | Age | Twin_status | Twin_Sibling | Zoster | HSV1 | HSV2 | CMV | Antibody (D28/D0) | ELISPOT (D28/D0) |
|------------|--------|-----|----------------|--------------|----------|----------|----------|----------|-------------------|------------------|
| A1 | Male | 52 | Identical twin | A2 | No | negative | negative | negative | 5.66 | 4.57 |
| A2 | Male | 52 | Identical twin | A1 | No | positive | negative | negative | 1.04 | 3.89 |
| B1 | Female | 58 | Identical twin | B2 | No | negative | negative | positive | 1.48 | N.D. |
| B2 | Female | 58 | Identical twin | B1 | no | negative | negative | negative | 3.2 | 2.40 |
| C1 | Female | 57 | Identical twin | C2 | no | negative | positive | negative | 4.92 | 5.99 |
| C2 | Female | 57 | Identical twin | C1 | no | negative | negative | positive | >10 | 6.85 |
| D | Male | 55 | Non-twin | | no | positive | negative | positive | 2.23 | 5.61 |
| E | Male | 75 | Non-twin | | >5 years | positive | negative | negative | >10 | 1.68 |
| F | Male | 60 | Non-twin | | no | negative | negative | positive | 3.37 | 5.69 |

Table S2. Number of TRB sequence reads obtained for individual replicates.

| VZV-specific CD4 T cells | Subject ID | Day 0 | Day 0 | Day 0 | Day 8 | Day 8 | Day 8 | Day 14 | Day 14 | Day 14 | Day 28 | Day 28 | Day 28 |
|--------------------------|------------|-------|-------|-------|-------|-------|-------|--------|--------|--------|--------|--------|--------|
| | | L1 | L2 | L3 | L1 | L2 | L3 | L1 | L2 | L3 | L1 | L2 | L3 |
| | A1 | 48695 | 57633 | 48716 | 59732 | 53081 | 42513 | 53294 | 50904 | 51965 | 62741 | 64280 | 62849 |
| | A2 | 58076 | 59575 | 54089 | 60881 | 60012 | 64411 | 60677 | 55149 | 58241 | 65310 | 60867 | 60069 |
| | B1 | 47391 | 59401 | 52956 | 43023 | 47453 | 50177 | 49698 | 47818 | 44815 | 43212 | 39879 | 41288 |
| | B2 | 46941 | 45472 | 47035 | 44366 | 45691 | - | 45487 | 48536 | 52138 | 47767 | - | - |
| | C1 | 57353 | 61798 | 60348 | 59435 | 51922 | 56616 | 67634 | 68780 | 68230 | 63041 | 63572 | 58650 |
| | C2 | 62122 | 67081 | 66718 | 76838 | 71034 | 69057 | 69088 | 56647 | 65190 | 62144 | 68341 | - |
| | D | 47208 | 46804 | 47735 | 52346 | 54221 | 50207 | 39540 | 49646 | 51417 | 51643 | 54449 | 58415 |
| | E | 78715 | 88679 | - | 90600 | 75731 | 71436 | 74851 | 70089 | 80839 | 80449 | 75447 | 87440 |
| | F | 43190 | 56208 | 53529 | 59691 | 51390 | 54116 | 66700 | 60754 | 67888 | 48977 | 59206 | 48032 |

| Total CD4 T cells | Subject ID | Day 0 | Day 0 | Day 8 | Day 8 | Day 14 | Day 14 | Day 28 | Day 28 |
|--------------------------|------------|--------|--------|--------|--------|--------|--------|--------|--------|
| | A1 | 222406 | 205464 | 234247 | 235525 | 250567 | 253631 | 274945 | 269052 |
| | A2 | 210203 | 229380 | 279221 | 274866 | 285546 | 291564 | 249733 | 326067 |
| | B1 | 431852 | 398666 | 398520 | 414006 | 429836 | 416636 | 381954 | 385298 |
| | B2 | 380704 | 368087 | 417171 | 417837 | 396486 | 410511 | 412817 | 406971 |
| | C1 | 333912 | 384750 | 477405 | 401121 | 416192 | 354103 | 412915 | 443915 |
| | C2 | 376250 | 436517 | 391237 | 429679 | 388229 | 386030 | 420384 | 403174 |
| | D | 388874 | 432311 | 415786 | 427977 | 464124 | 459797 | 443345 | 403249 |
| | E | 376809 | 399194 | 378732 | 438010 | 442264 | 483192 | 393922 | 374185 |
| | F | 361072 | 392749 | 398108 | 458999 | 370432 | 401485 | 335422 | 278238 |
| | | | | | | | | | |
| CD4 T cell subsets day 0 | Subject ID | Naïve | Naïve | Memory | Memory | | | | |
| | A1 | 630202 | | 647555 | | | | | |
| | A2 | 306913 | 287861 | 152222 | 163975 | | | | |
| | B1 | 417332 | | 420268 | | | | | |
| | B2 | 431890 | | 461370 | | | | | |
| | C1 | 319468 | | 287179 | | | | | |
| | C2 | 271646 | 304954 | 291309 | 296227 | | | | |
| | D | 406796 | | 397015 | | | | | |
| | E | 262911 | | 356331 | | | | | |
| | F | 650645 | | 632600 | | | | | |

Table S3. BV and BJ gene segment usage in VZV-reactive CD4 T cells compared to naïve and memory CD4 T cells (FDR \leq 0.1).

| Increase | Naïve CD4 T cells | Memory CD4 T cells |
|----------|-------------------|--------------------|
| TRBV5-4 | 0.004* | Non-significant |
| TRBV5-5 | 0.02 | Non-significant |
| TRBV5-8 | 0.027 | 0.008 |
| TRBV6-1 | 0.02 | Non-significant |
| TRBV7-3 | 0.02 | 0.02 |
| TRBV7-4 | 0.012 | 0.02 |
| TRBV12-4 | 0.004 | 0.004 |
| Decrease | Naïve CD4 T cells | Memory CD4 T cells |
| TRBV10-3 | 0.008 | 0.012 |
| TRBV14 | 0.008 | 0.008 |
| TRBV15 | 0.012 | 0.004 |
| TRBV19 | 0.004 | 0.012 |
| TRBV20-1 | 0.004 | 0.004 |
| TRBV4-3 | 0.004 | 0.004 |
| TRBV5-3 | 0.022 | 0.004 |
| TRBJ1-4 | Non-significant | 0.008 |
| TRBJ1-5 | Non-significant | 0.02 |
| TRBJ2-1 | 0.004 | 0.004 |

* Only comparisons that were significantly different are shown. Data are shown as p-values with FDR \leq 0.1 based on Benjamini Hochberg adjustment.

Table S4. Serum cytokine levels before and one day after vaccination (mean fluorescence intensity)

| Subject ID | B1 | B1 | B2 | B2 | C1 | C1 | C2 | C2 | D | D | E | E | F | F |
|------------|------|------|------|------|------|------|------|------|------|------|------|------|------|------|
| Visit | D0 | D1 | D0 | D1 | D0 | D1 | D0 | D1 | D0 | D1 | D0 | D1 | D0 | D1 |
| IL17F | 88 | 91 | 112 | 114 | 226 | 260 | 371 | 391 | 56 | 57 | 55 | 58 | 207 | 201 |
| FASL | 46 | 46 | 52 | 54 | 38 | 42 | 105 | 108 | 33 | 33 | 37 | 35 | 92 | 89 |
| TGFA | 26 | 24 | 28 | 25 | 59 | 68 | 53 | 64 | 21 | 22 | 24 | 23 | 35 | 31 |
| MIP1A | 103 | 100 | 171 | 184 | 159 | 178 | 690 | 779 | 62 | 57 | 72 | 67 | 371 | 364 |
| SDF1A | 218 | 209 | 191 | 199 | 310 | 337 | 223 | 272 | 175 | 178 | 180 | 169 | 202 | 195 |
| IL27 | 29 | 31 | 36 | 35 | 27 | 28 | 56 | 63 | 27 | 26 | 25 | 26 | 55 | 52 |
| LIF | 46 | 51 | 60 | 60 | 39 | 41 | 113 | 125 | 41 | 42 | 45 | 45 | 61 | 71 |
| IL1B | 15 | 18 | 22 | 22 | 17 | 18 | 26 | 31 | 17 | 18 | 20 | 19 | 23 | 22 |
| IL2 | 21 | 20 | 25 | 24 | 17 | 17 | 56 | 58 | 16 | 18 | 19 | 20 | 40 | 38 |
| IL4 | 89 | 90 | 86 | 91 | 89 | 91 | 117 | 129 | 96 | 91 | 126 | 116 | 116 | 114 |
| IL5 | 30 | 34 | 31 | 32 | 23 | 23 | 82 | 91 | 26 | 26 | 25 | 26 | 57 | 59 |
| IP10 | 91 | 124 | 125 | 371 | 49 | 78 | 51 | 937 | 63 | 72 | 170 | 196 | 91 | 92 |
| IL6 | 33 | 35 | 39 | 40 | 31 | 32 | 65 | 72 | 29 | 31 | 29 | 31 | 46 | 44 |
| IL7 | 271 | 295 | 238 | 245 | 491 | 502 | 445 | 515 | 544 | 586 | 905 | 946 | 715 | 609 |
| IL8 | 50 | 48 | 66 | 67 | 52 | 59 | 57 | 62 | 48 | 49 | 48 | 45 | 78 | 66 |
| IL10 | 35 | 34 | 30 | 29 | 16 | 16 | 88 | 112 | 16 | 16 | 17 | 19 | 42 | 41 |
| PIGF1 | 224 | 216 | 202 | 204 | 338 | 355 | 289 | 290 | 158 | 160 | 208 | 201 | 244 | 243 |
| IFNB | 98 | 102 | 117 | 125 | 305 | 348 | 404 | 469 | 78 | 77 | 80 | 79 | 233 | 227 |
| EOTAXIN | 76 | 63 | 161 | 185 | 174 | 231 | 320 | 364 | 239 | 196 | 149 | 107 | 379 | 365 |
| IL12P70 | 27 | 25 | 36 | 40 | 33 | 34 | 61 | 108 | 30 | 30 | 34 | 34 | 63 | 60 |
| IL13 | 30 | 30 | 32 | 36 | 29 | 32 | 39 | 44 | 33 | 32 | 38 | 36 | 37 | 36 |
| IL17A | 62 | 64 | 55 | 56 | 35 | 38 | 50 | 55 | 40 | 40 | 35 | 34 | 84 | 80 |
| IL31 | 27 | 27 | 30 | 32 | 35 | 36 | 36 | 33 | 27 | 24 | 28 | 25 | 43 | 42 |
| IL1RA | 28 | 30 | 34 | 34 | 25 | 26 | 37 | 108 | 21 | 24 | 33 | 35 | 32 | 31 |
| SCF | 12 | 12 | 77 | 75 | 11 | 11 | 363 | 417 | 16 | 16 | 27 | 26 | 20 | 19 |
| RANTES | 1999 | 1904 | 2435 | 2354 | 2635 | 2695 | 2358 | 2009 | 1550 | 1545 | 1794 | 1590 | 2813 | 2876 |
| IFNG | 37 | 38 | 61 | 67 | 46 | 55 | 69 | 200 | 54 | 51 | 68 | 69 | 63 | 59 |
| GMCSF | 6220 | 6167 | 3299 | 3792 | 2091 | 2631 | 1497 | 2436 | 4198 | 3689 | 5659 | 5147 | 3785 | 4123 |
| TNFA | 322 | 314 | 312 | 323 | 317 | 317 | 311 | 347 | 325 | 316 | 368 | 351 | 316 | 314 |
| HGF | 178 | 172 | 112 | 119 | 179 | 182 | 174 | 253 | 194 | 187 | 331 | 270 | 295 | 279 |
| MIP1B | 107 | 95 | 570 | 609 | 151 | 170 | 142 | 215 | 74 | 74 | 73 | 71 | 77 | 75 |
| IFNA | 166 | 158 | 189 | 188 | 178 | 187 | 213 | 227 | 182 | 177 | 178 | 176 | 223 | 212 |
| TGFB | 68 | 70 | 120 | 118 | 106 | 102 | 170 | 189 | 120 | 104 | 114 | 114 | 94 | 92 |
| MCP1 | 606 | 632 | 578 | 749 | 429 | 554 | 405 | 2332 | 1116 | 985 | 751 | 739 | 1611 | 1540 |
| IL9 | 76 | 77 | 97 | 99 | 68 | 71 | 101 | 104 | 70 | 72 | 72 | 69 | 117 | 113 |
| VEGFD | 56 | 61 | 42 | 43 | 39 | 38 | 65 | 74 | 48 | 51 | 61 | 59 | 64 | 60 |
| TNFB | 78 | 80 | 97 | 100 | 98 | 102 | 162 | 160 | 90 | 93 | 96 | 91 | 161 | 154 |
| NGF | 20 | 24 | 27 | 28 | 18 | 17 | 26 | 31 | 21 | 22 | 18 | 20 | 22 | 22 |
| EGF | 136 | 98 | 78 | 115 | 237 | 486 | 1391 | 901 | 1079 | 509 | 1527 | 672 | 91 | 117 |
| BDNF | 3485 | 3359 | 3747 | 4017 | 4404 | 5203 | 4861 | 4152 | 6740 | 6523 | 7960 | 7081 | 2494 | 2563 |
| TRAIL | 163 | 153 | 147 | 143 | 254 | 290 | 110 | 130 | 71 | 73 | 76 | 74 | 76 | 74 |
| GCSF | 88 | 90 | 88 | 102 | 84 | 90 | 148 | 208 | 103 | 101 | 100 | 97 | 138 | 133 |
| GROA | 32 | 33 | 40 | 41 | 36 | 39 | 42 | 45 | 32 | 30 | 32 | 30 | 44 | 41 |
| IL1A | 110 | 103 | 98 | 100 | 195 | 211 | 122 | 123 | 72 | 70 | 95 | 90 | 112 | 112 |
| IL23 | 25 | 23 | 26 | 25 | 25 | 27 | 31 | 34 | 23 | 25 | 24 | 22 | 32 | 32 |
| IL12P40 | 444 | 436 | 517 | 551 | 678 | 735 | 492 | 606 | 566 | 532 | 796 | 745 | 664 | 650 |

| | | | | | | | | | | | | | | |
|----------|-------|-------|-------|-------|-------|-------|-------|-------|-------|-------|-------|-------|-------|-------|
| IL15 | 43 | 41 | 38 | 38 | 32 | 35 | 79 | 84 | 33 | 36 | 39 | 39 | 67 | 63 |
| IL18 | 211 | 207 | 222 | 230 | 308 | 321 | 347 | 378 | 201 | 187 | 378 | 374 | 234 | 232 |
| MCSF | 37 | 39 | 45 | 45 | 39 | 40 | 52 | 52 | 33 | 34 | 35 | 32 | 53 | 50 |
| MCP3 | 50 | 57 | 53 | 61 | 56 | 59 | 54 | 65 | 57 | 58 | 48 | 52 | 58 | 63 |
| MIG | 76 | 82 | 63 | 72 | 138 | 160 | 93 | 583 | 48 | 49 | 105 | 106 | 63 | 63 |
| RESISTIN | 4024 | 3576 | 2662 | 3014 | 2275 | 2280 | 3374 | 4572 | 2387 | 2505 | 4969 | 4280 | 3709 | 3060 |
| IL21 | 48 | 47 | 40 | 37 | 118 | 126 | 56 | 65 | 28 | 29 | 30 | 30 | 33 | 34 |
| ICAM1 | 1002 | 973 | 935 | 1019 | 1996 | 1956 | 942 | 1104 | 1959 | 1857 | 3049 | 2882 | 1907 | 1835 |
| VCAM1 | 17279 | 17216 | 16949 | 17093 | 16881 | 16878 | 16501 | 16621 | 17114 | 16952 | 17708 | 17570 | 17212 | 17398 |
| FGFB | 39 | 37 | 47 | 50 | 29 | 31 | 77 | 81 | 34 | 33 | 36 | 34 | 72 | 71 |
| IL22 | 44 | 83 | 66 | 64 | 54 | 59 | 61 | 96 | 105 | 78 | 425 | 119 | 51 | 86 |
| PDGFBB | 54 | 60 | 42 | 42 | 147 | 145 | 140 | 145 | 192 | 230 | 730 | 864 | 231 | 173 |
| VEGF | 222 | 212 | 152 | 156 | 281 | 331 | 210 | 309 | 415 | 399 | 293 | 270 | 404 | 380 |
| LEPTIN | 3601 | 3417 | 1401 | 1676 | 961 | 1272 | 584 | 1207 | 2776 | 2598 | 3426 | 3202 | 2431 | 2769 |
| PAI1 | 10933 | 10775 | 11385 | 11538 | 11608 | 11636 | 11287 | 11009 | 11690 | 11656 | 12171 | 11947 | 11361 | 11897 |
| CD40L | 197 | 167 | 239 | 278 | 239 | 286 | 992 | 1037 | 156 | 126 | 251 | 163 | 694 | 711 |
| ENA78 | 595 | 551 | 550 | 569 | 355 | 339 | 123 | 95 | 263 | 230 | 169 | 162 | 530 | 459 |
| CHEX1 | 11335 | 11816 | 11569 | 11375 | 11304 | 11996 | 11199 | 11660 | 11625 | 11604 | 11667 | 11737 | 11457 | 11606 |
| CHEX2 | 1003 | 915 | 1184 | 1082 | 1249 | 1333 | 1232 | 1314 | 1171 | 1173 | 1174 | 1075 | 449 | 1341 |
| CHEX3 | 607 | 591 | 555 | 579 | 625 | 629 | 663 | 677 | 578 | 609 | 623 | 588 | 584 | 663 |
| CHEX4 | 32 | 46 | 49 | 45 | 23 | 23 | 22 | 27 | 29 | 31 | 27 | 31 | 14 | 16 |

Table S5. Frequencies of VZV antigen-reactive TCR β chain sequences in total CD4 T cells (%)

| Subject ID | A1 | | A2 | | B1 | | B2 | | C1 | | C2 | | D | | E | | F | |
|------------|------|------|------|------|------|------|------|------|------|------|------|------|------|------|------|------|------|------|
| Day 0 | 0.25 | 0.24 | 0.19 | 0.18 | 0.26 | 0.27 | 0.12 | 0.09 | 0.34 | 0.35 | 0.47 | 0.58 | 0.30 | 0.33 | 0.68 | 0.67 | 0.55 | 0.52 |
| Day 8 | 1.49 | 1.49 | 0.50 | 0.57 | 1.41 | 1.37 | 0.48 | 0.48 | 0.76 | 0.79 | 3.08 | 3.37 | 1.54 | 1.60 | 1.17 | 1.09 | 1.01 | 1.08 |
| Day 14 | 1.18 | 1.21 | 0.58 | 0.66 | 1.01 | 1.04 | 0.87 | 0.82 | 0.73 | 0.71 | 2.07 | 2.13 | 1.00 | 0.98 | 0.97 | 0.91 | 1.11 | 1.11 |
| Day 28 | 0.69 | 0.66 | 0.49 | 0.51 | 0.67 | 0.74 | 0.64 | 0.68 | 0.70 | 0.73 | 1.07 | 1.07 | 0.54 | 0.52 | 0.86 | 0.84 | 0.82 | 0.98 |

Two replicates of one million ex vivo total CD4 T cells were sequenced for each individual at each time point and examine for the presence and frequencies of TCR β chain sequences from VZV-reactive T cells. Summary metrics is shown in Figure 3A.

Table S6. Clonal sizes of VZV antigen-reactive CD4 T cells derived from naïve or memory cells (#reads/million reads)

| Naïve derived | Subject ID | A1 | A2 | B1 | B2 | C1 | C2 | D | E | F |
|----------------|------------|-------|-------|-------|-------|-------|-------|-------|-------|-------|
| | Day 0 | 0.00 | 2.77 | 13.71 | 0.00 | 5.95 | 8.44 | 4.07 | 4.93 | 2.93 |
| | Day 8 | 2.57 | 9.46 | 20.18 | 7.74 | 9.36 | 16.32 | 19.12 | 6.48 | 3.67 |
| | Day 14 | 4.83 | 9.68 | 22.68 | 24.10 | 4.92 | 12.61 | 9.74 | 6.27 | 3.98 |
| | Day 28 | 6.71 | 9.41 | 13.86 | 44.11 | 7.28 | 5.91 | 8.78 | 5.44 | 7.72 |
| Memory derived | Subject ID | A1 | A2 | B1 | B2 | C1 | C2 | D | E | F |
| | Day 0 | 12.79 | 12.23 | 9.39 | 11.84 | 12.65 | 10.19 | 9.34 | 18.33 | 13.23 |
| | Day 8 | 49.32 | 20.53 | 33.56 | 37.03 | 20.53 | 47.55 | 28.71 | 26.14 | 15.28 |
| | Day 14 | 39.06 | 22.52 | 23.61 | 52.44 | 18.34 | 31.72 | 17.08 | 21.58 | 15.45 |
| | Day 28 | 23.36 | 19.47 | 20.38 | 43.10 | 18.08 | 16.08 | 10.94 | 19.68 | 14.92 |

Summary metrics is shown in Figure 4C.

Table S7. Diversity of VZV-specific CD4 TCR repertoire

| Number of clones | Subject ID | Day 0 | Day 28 |
|-------------------|------------|-------|--------|
| | A1 | 83 | 96 |
| | A2 | 68 | 65 |
| | B1 | 166 | 219 |
| | B2 | 50 | 78 |
| | C1 | 150 | 220 |
| | C2 | 230 | 260 |
| | D | 155 | 206 |
| | E | 120 | 140 |
| | F | 194 | 365 |
| Percent of clones | Subject ID | Day 0 | Day 28 |
| | A1 | 0.05 | 0.06 |
| | A2 | 0.07 | 0.07 |
| | B1 | 0.07 | 0.09 |
| | B2 | 0.07 | 0.11 |
| | C1 | 0.06 | 0.08 |
| | C2 | 0.09 | 0.11 |
| | D | 0.06 | 0.08 |
| | E | 0.10 | 0.11 |
| | F | 0.06 | 0.11 |

The diversity index was calculated as described in Figure 5A and is expressed as either the number or the percent of the largest clones that take up 80% of the repertoire space. Summary metrics are shown in Figures 5B and C.

Supplementary Figures

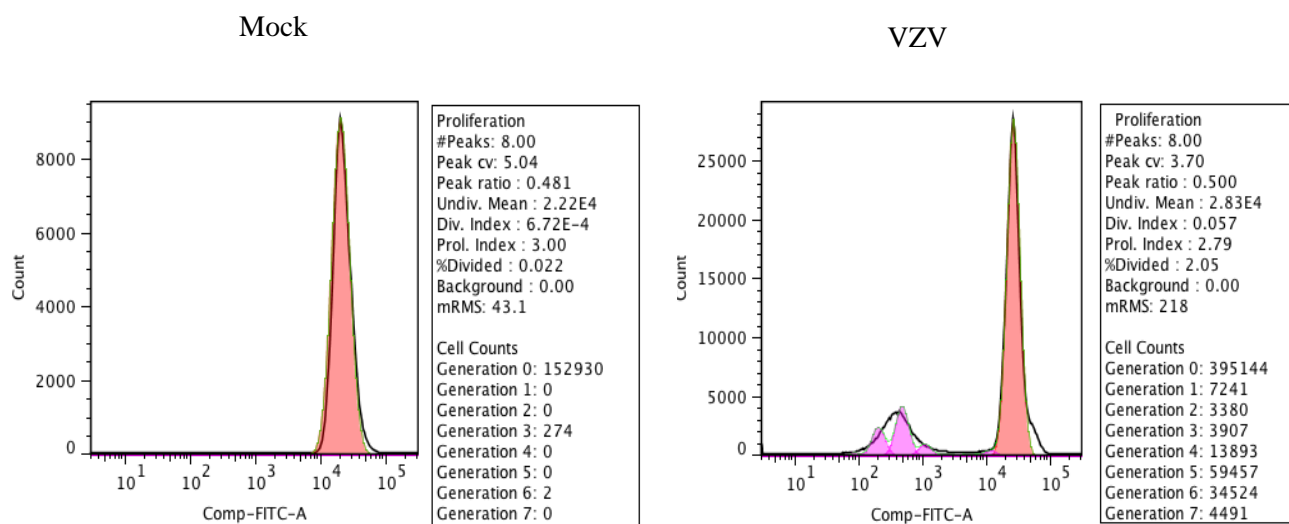


Fig. S1. VZV lysate-induced T cell proliferation. CFSE-labeled PBMCs were stimulated with VZV lysate or mock lysate for 8 days as described in Fig. 1a. The figure of gated CD4 T cells shows the data analysis using the FlowJo Proliferation Platform shows with number of cell division and cell numbers in each generation.

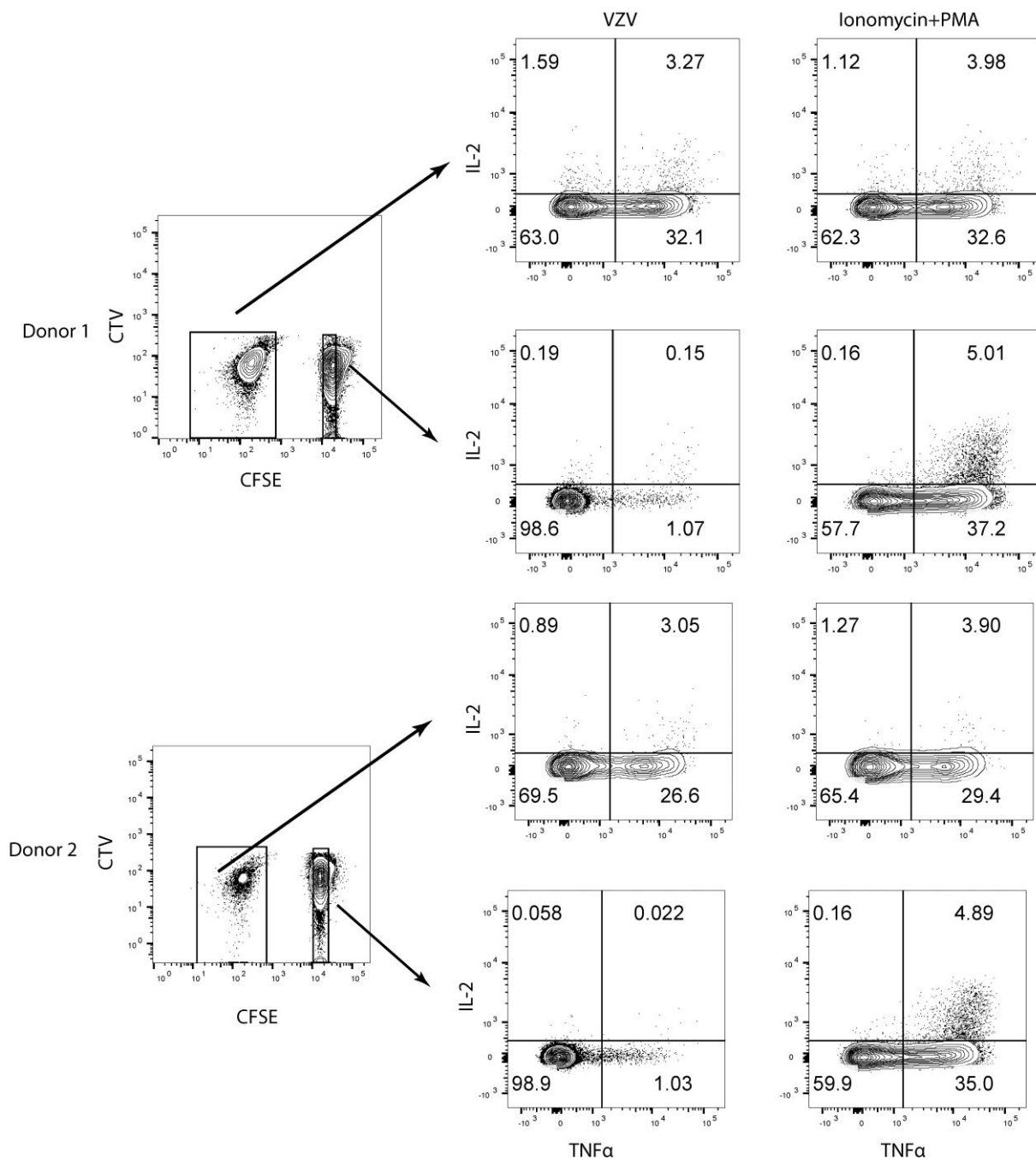


Fig. S2. Cytokine production of VZV-antigen reactive CD4 T cells. 8-day VZV lysate-activated CFSE-labeled PBMCs were restimulated by either PMA and ionomycin or VZV lysate together with fresh CTV-T cell-depleted PBMCs. CFSE low and CFSE high CTV-negative CD4 T cells were gated and plotted for TNF α and IL-2. Cytokine production in VZV antigen- and ionomycin/PMA-stimulated cells were compared and the fraction of cytokine-producing cells stimulated by VZV lysate after normalization for the number of cytokine-producing cells after stimulation with PMA and ionomycin is shown in Figure 1b.

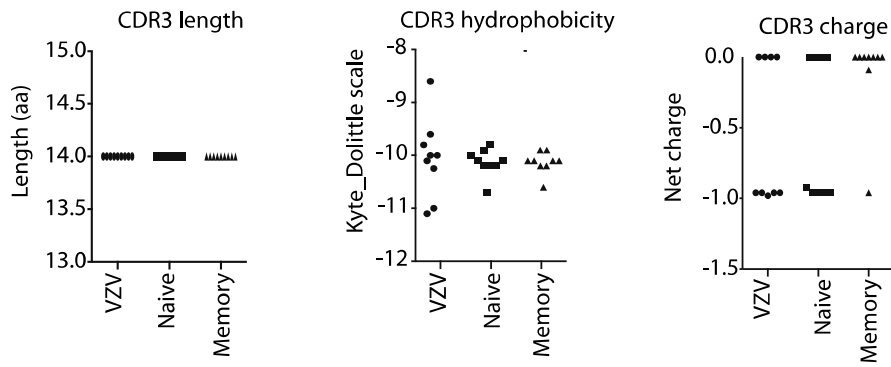


Fig. S3. CDR3 features of VZV antigen-reactive CD4 T cells. The median length (left panel), hydrophobicity (middle panel) and net charge (right panel) of CDR3 amino acid sequences in VZV-reactive, naïve and memory CD4 TCR β repertoires are compared using paired Wilcoxon-Mann-Whitney test.